

Articles

Kinetics and Mass Transfer of Organic Liquid-Phase Reactions in the Presence of a Sparingly Soluble Solid Phase

Esko Tirronen,[†] Tapio Salmi,^{*‡} Juha Lehtonen,[§] Antti Vuori,[†] Outi Grönfors,[†] and Kai Kaljula[‡]

Kemira Agro Oy, Espoo Research Centre, P.O. BOX 44, FIN-22071 Espoo, Finland, Åbo Akademi, Process Chemistry Group, Laboratory of Industrial Chemistry, FIN-20500 Turku-Åbo, Finland, and Neste Engineering, P.O. BOX 310, FIN-06191, Porvoo, Finland

Abstract:

Several organic liquid-phase reactions are carried out in the presence of a sparingly soluble reactive solid phase which is gradually dissolved during the course of the reaction. The presence of the reactive solid phase complicates the treatment of kinetic data, since the overall reaction rate is influenced by the solubility equilibrium and mass transfer rate of the solid compound. A mathematical model has been derived for an organic reaction system with one reactive solid compound. The modelling concept was applied on a linear multistep reaction system, Claisen condensation. The solubility of the solid compound was measured with batch experiments carried out under nonreactive conditions, and the kinetic parameters for the reaction system were determined from the data obtained by semibatch experiments. Model simulations clarified the behavior of the sparingly soluble reactive compound in the process, indicating that the rate equations describe well the experimental kinetic data.

Introduction

This contribution considers the production of organic fine chemicals in the presence of a sparingly soluble reactive solid phase. The key factors in modelling of such processes involve the reaction mechanism and kinetics, the dissolution rates, the solubility equilibria as well as the global mass balance equations for the liquid and solid phases. Herein we consider stepwise organic processes using one sparingly soluble reactive compound. Rate equations for consecutive linear reaction mechanisms are derived and applied on liquid–solid processes proceeding in an ideally mixed isothermal semi-batch reactor. The applicability of the general procedure is illustrated with a Claisen condensation reaction. The mathematical model can be used for scale-up of Claisen condensation.

Reaction Mechanism and Rate equations. Several liquid-phase organic reactions have been applied in the presence of a reactive, but sparingly soluble solid compound.

The presence of a solid compound strongly affects the reaction kinetics since the effective liquid-phase concentration of the solid compound is limited by its solubility. A typical example is Claisen condensation reaction in the presence of alkoxide. The formal mechanism of Claisen condensation for this actual case is described in Scheme 1.

Claisen condensation between an ester and a ketone proceeds via the mechanism described in Scheme 1. For a quantitative treatment of the kinetics, the reaction mechanism can be compressed to a four-step process. The reaction is initiated by a proton removal with methoxide from the α -carbon atom of the ketone. Methanol and a carbanion are formed in this step (step 1). The carbanion attacks the carbonyl group of the ester (step 2). The last steps (steps 3 and 4) involve methoxide elimination and charge distribution between tautomeric keto- and enol forms of D. The parallel route (steps 5 and 6) yielding acetophenone (G) is distinctively less favored compared to step 4. To simplify the development of the kinetic model, these steps (steps 5 and 6) are excluded from the main reaction scheme since the concentration of G in the reaction mixture was found to be very small and inconsistent.

On the basis of the simplified treatment of the reaction pathway, the elementary steps leading to the formation of the final product (D) and methanol (E) can be compressed as follows:



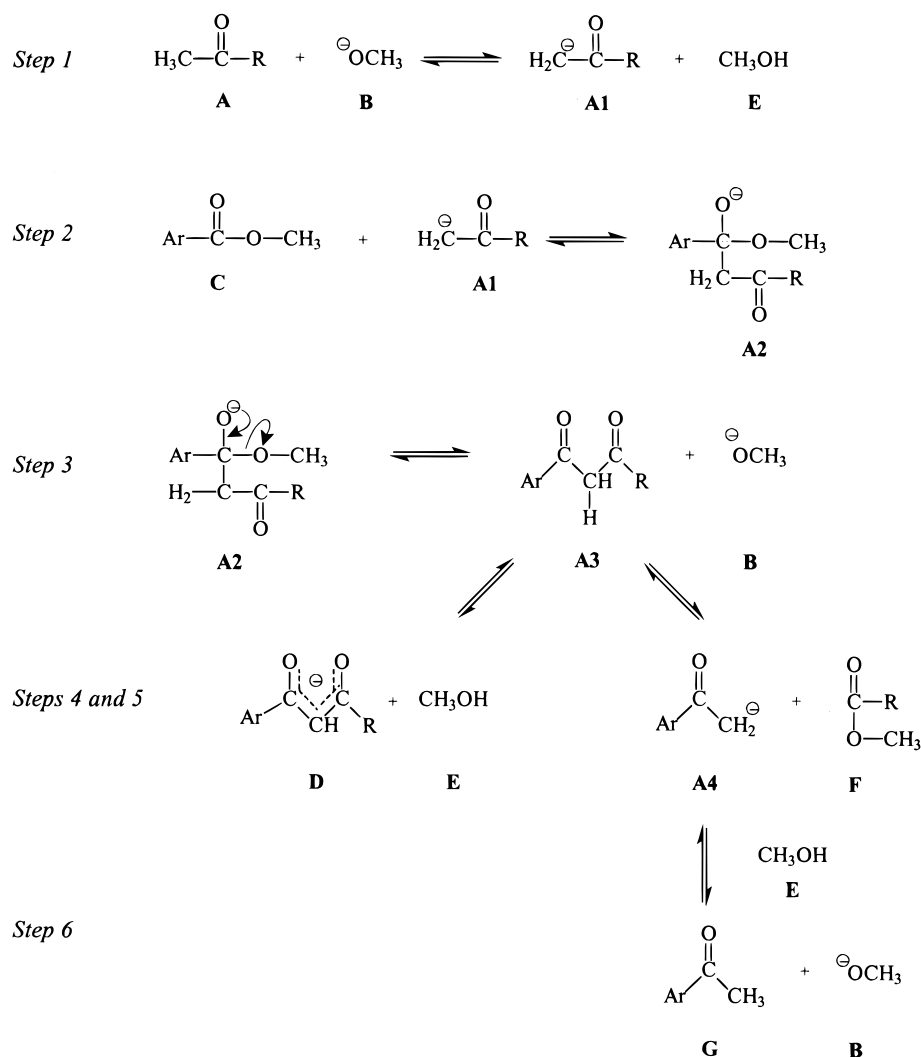
where A, B, C, D, and E are analytically detectable compounds and A1, A2, and A3 are the reaction intermediates that is, the carbanions. The mechanism, eqs 1–4 is linear with respect to the intermediates, since the intermediates always react with a compound detectable by chemical analysis (B and C). This fact essentially simplifies the derivation

[†] Kemira Agro Oy, Espoo Research Centre.

[‡] Åbo Akademi, Process Chemistry Group, Laboratory of Industrial Chemistry.

[§] Neste Engineering.

Scheme 1. Reaction scheme of Claisen condensation



of the rate equation for the overall process. The concentrations of the intermediates can be solved analytically from the condition of a quasi-steady state. The quasi-steady-state hypothesis implies that the generation rate of intermediates is approximated to zero.^{4,5} Applying the quasi-steady-state hypothesis on the reactive intermediates (A1, A2, and A3) gives the generation rates for the compounds

$$r_{A1} = r_1 - r_2 = 0 \quad (5a)$$

$$r_{A2} = r_2 - r_3 = 0 \quad (5b)$$

$$r_{A3} = r_3 - r_4 = 0 \quad (5c)$$

where r_1, \dots, r_4 denote the velocities of steps 1–4.

- (1) Haario, H. *MODEST-User's Guide*; Profmath Oy: Helsinki, 1994.
- (2) Hindmarsh, A. C. *A Systematized Collection of Ode-Solvers in Scientific Computing*; Steple, R., et al., Eds.; IMACS North-Holland: Amsterdam, 1983; pp 55–64.
- (3) Marquardt, D. W. An Algorithm for Least Squares Estimation on Nonlinear Parameters. *SIAM J.* **1963**, 431–441.
- (4) Boudart, M. *Kinetics of Chemical Processes*; Prentice Hall Inc.: Englewood Cliffs, N.J., 1968; pp 67–70.
- (5) Laidler, K. J. *Chemical Kinetics*; Harper & Collins: New York, 1987; p 282.

Conditions 5a–5c imply that the overall rate is equal to $r = r_1 = r_2 = r_3 = r_4$.

Provided that steps 1–4 represent elementary reactions, their rates can be written as

$$r_1 = k_1 \left(c_A c_B - \frac{c_{A1} c_E}{K_1} \right) = a_1 - a_{-1} c_{A1} = r \quad (6)$$

$$r_2 = k_2 \left(c_{A1} c_C - \frac{c_{A2}}{K_2} \right) = a_2 c_{A1} - a_{-2} c_{A2} = r \quad (7)$$

$$r_3 = k_3 \left(c_{A2} - \frac{c_{A3} c_B}{K_3} \right) = a_3 c_{A2} - a_{-3} c_{A3} = r \quad (8)$$

$$r_4 = k_4 \left(c_{A3} c_B - \frac{c_D c_E}{K_4} \right) = a_4 c_{A3} - a_{-4} = r \quad (9)$$

The principle of the derivation of the global rate equations is to eliminate the concentrations of highly reactive carban-

- (6) Haario, H.; Kalachev, L. Asymptotic Analysis of A Complex Consecutive Reaction Scheme. Manuscript submitted.
- (7) Green, J.; Margerison, D. *Statistical Treatment of Experimental Data*; Elsevier Scientific Publishing Company: Amsterdam–Oxford–New York, 1978; Chapter 5.

ions (A1, A2, and A3). The concentrations of A1 and A3 are solved from eqs 6 and 9 giving

$$c_{A1} = \frac{a_1}{a_{-1}} - \frac{r}{a_{-1}} \quad (10)$$

$$c_{A3} = \frac{a_{-4}}{a_4} - \frac{r}{a_4} \quad (11)$$

Adding eqs 7 and 8 allows the elimination of c_{A2}

$$(a_3 + a_{-2})r = a_2 a_3 c_{A1} - a_{-2} a_{-3} c_{A3} \quad (12)$$

Equations 10 and 11 are introduced into 12 from which the rate r is solved:

$$r = \frac{a_1 a_2 a_3 a_4 - a_{-1} a_{-2} a_{-3} a_{-4}}{a_{-1} a_{-2} a_{-3} + a_{-1} a_{-2} a_4 + a_{-1} a_3 a_4 + a_2 a_3 a_4} \quad (13)$$

where the original notations for the factors a_1, \dots, a_4 and a_{-1}, \dots, a_{-4} are given in the Appendix.

After introducing the rate and equilibrium constants into eq 13, the following rate equation is obtained:

$$r = \frac{k_1 k_2 k_3 k_4 c_A c_B c_C - \frac{k_1 k_2 k_3 k_4}{K_1 K_2 K_3 K_4} c_B c_E c_D}{\frac{k_1 k_2 k_3 c_B c_E}{K_1 K_2 K_3} + \frac{k_1 k_2 k_4 c_B c_E}{K_1 K_2} + \frac{k_1 k_3 k_4 c_B c_E}{K_1} + k_2 k_3 k_4 c_B c_C} \quad (14)$$

The rate eq 14 can be rewritten by using a lumped overall rate constant $k = \prod_{j=1}^4 k_j$ and an overall equilibrium constant $K = \prod_{j=1}^4 K_j$:

$$r = \frac{k \left(c_A c_B c_C - \frac{c_E c_D}{K} \right)}{k_2 k_3 k_4 c_C + \left(\frac{k_2 k_3}{K_2 K_3} + \frac{k_2 k_4}{K_2} + k_3 k_4 \right) \frac{k_1 c_E}{K_1}} \quad (15)$$

Generalization of the Rate Equation. The rate eq 15 can be expressed in a more general form by introducing merged parameters K' and K'' defined as follows:

$$K' = k_2 k_3 k_4 \quad \text{and} \quad K'' = \frac{\left(\frac{k_2 k_3}{K_2 K_3} + \frac{k_2 k_4}{K_2} + k_3 k_4 \right) k_1}{K_1} \quad (16)$$

that is

$$r = \frac{k \left(c_A c_B c_C - \frac{c_E c_D}{K} \right)}{K' c_C + K'' c_E} \quad (17)$$

Claisen condensation can be regarded practically as an irreversible process (K is large); thus, the rate eq 17 approaches the expression

$$r = \frac{k c_A c_B c_C}{K' c_C + K'' c_E} \quad (18)$$

which is the form in which the kinetic equation can be applied in practical modelling.

Depending upon the magnitudes of K' and K'' , we can obtain equations which are proportional to $c_A c_B$ or $c_A c_B c_C / c_E$ in extreme cases.

The rate constants are assumed to be dependent on temperature according to Arrhenius' law:

$$k_j = k_j(T_0) \exp\left(-\frac{E_j}{R_g} \left(\frac{1}{T} - \frac{1}{T_0}\right)\right) \quad (19)$$

where T_0 is a reference temperature, typically an average temperature of the kinetic experiments. The transformed form, eq 19 was applied in order to suppress the mutual correlation of the pre-exponential factor and the activation energy in the estimation of kinetic parameters.

Side Reactions

Some side reactions may be taken into account as illustrated in Scheme 2. A simplified kinetic treatment was applied for these side reactions.

Side Reactions S1–S3. The water (S11) present in the reaction system reacts with methoxide (B) giving hydroxide (S12) and methanol (E). The hydroxide (S12) saponifies the ester (C), giving carboxylic acid (S21) and methanol (E). The ester (C) reacts with methoxide (B) yielding carboxylic acid (S21) and dimethyl ether (S31). Since methoxide is highly hydroscopic and prone to adsorb moisture from the air, it inevitably contains varying amounts of hydroxide. While methoxide as well as hydroxide are sparingly soluble into chlorobenzene, their solubilities are remarkably enhanced in the presence methanol formed during the reaction. Due to unexpected amounts of hydroxide in the system and the fact that the water concentration equals ~ 0 , the consumption velocity of C and B can be expressed in a simplified lumped form:

$$r_{S2S3} = k_{S2S3} c_C c_B \quad (20)$$

Side Reaction S4. Side reaction S4 was not taken into account in the final set of the kinetic equations. The initial concentration of the dimethyl formamide (S41) was very low, and thus the expected change of the reaction products was not affected to any significant degree.

Side Reaction S5. Side reaction S5, the reaction of the ketone (A) with the methoxide (B) was excluded from the kinetic modelling. Since the amount of the products of this reaction were very low, they were difficult to measure accurately using gas chromatography (GC) even with a large excess of the reactant A.

Reactor Model, Mass Balance for Liquid-Phase Components

The rate equations appear in the mass balances of the compounds in the reactor. Organic reactions are typically carried out in semibatch reactors, that is, some of the compounds are initially charged into the reaction vessel, followed by addition of other materials. These procedures often require control of the temperature in the system. Otherwise, they might result in a run-away behavior, especially in the case of reactions involved with severe exotherm.

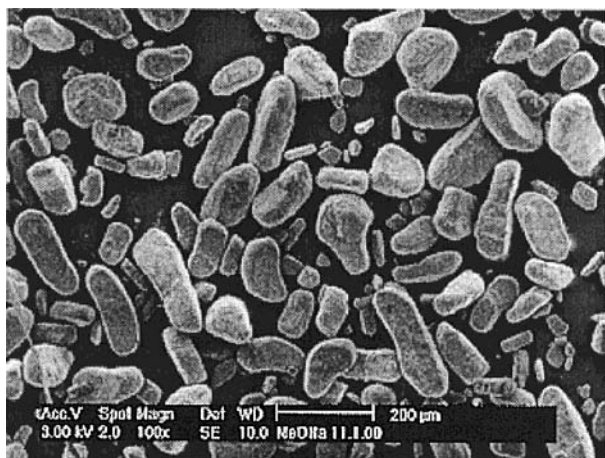


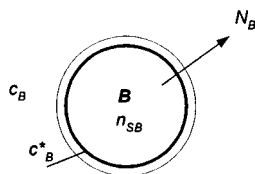
Figure 1. A SEM image of methoxide particles.

are obtained from the molar amounts and from the volume: $c_i = n_i/V$. The mass fractions are obtained from the concentrations and molecular weights of the compounds:

$$w_i = \frac{m_i}{\sum_j m_j} = \frac{n_i M_i}{\sum_j n_j M_j} = \frac{c_i M_i}{\sum_j c_j M_j}$$

Modelling Solid Compound Consumption

In a case where just one of the compounds (A) is fed into the reactor and one of the compounds (B, sodium methoxide) predominantly exists in the solid phase due to its limited solubility, the system is described below.



The interfacial flux of B is described with the Fick's law

$$N_B = k_{LB}(c_B^* - c_B) \quad (25)$$

where k_{LB} is the mass-transfer coefficient of B, while c_B^* and c_B denote the saturation and bulk-phase concentrations of B, respectively.

A SEM photograph of methoxide particles used in the kinetic experiments is presented in Figure 1.

When the solid particles are assumed to be of equal sizes, the molar amount of solid B is given by

$$n_{SB} = n_p \frac{\rho_{SB} V_p}{M_B} \quad (26)$$

where ρ_{SB} and M_B are the density and molar mass of B, respectively. V_p denotes the volume of the solid particle.

Differentiating eq 26 gives

$$\frac{dn_{SB}}{dt} = \frac{n_p \rho_{SB}}{M_B} \frac{dV_p}{dt} \quad (27)$$

The mass balance for solid B can be written as

$$\frac{dn_{SB}}{dt} = -N_B A \quad (28)$$

where A is the interfacial area.

For dissolved B, the mass balance in the liquid-phase becomes

$$\frac{dn_B}{dt} = r_B V + N_B A \quad (29)$$

Since B is sparingly soluble, it is possible to apply the pseudo-steady-state hypothesis to dissolved B, that is, $dn_B/dt = 0$. Addition of eqs 28 and 29 leads to the elimination of the interfacial flux and relates the consumption of solid B to its consumption rate:

$$\frac{dn_{SB}}{dt} = r_B V \quad (30)$$

When the expression for the particle volume, eq 27 is inserted in the mass balance (30), it is expressed as:

$$\frac{dV_p}{dt} = \frac{M_B}{\rho_{SB} n_p} r_B V \quad (31)$$

The further treatment of eq 31 is dependent on the geometry. For simple ideal geometries the derivatives are listed below

$$\begin{aligned} \frac{dV_p}{dt} &= 4\pi r'^2 \frac{dr'}{dt} \quad \text{for spheres} \\ &= 2\pi L r' \frac{dr'}{dt} \quad \text{for infinitely long cylinders} \\ &= 2L^2 \frac{dr'}{dt} \quad \text{for slabs} \end{aligned} \quad (32)$$

where r' denotes the radius of the sphere or the cylinder; for slabs r' is half-thickness of the slab; L is the length of the cylinder or L^2 is the area of the slab.

For spherical particles, the relationship 32 implies that we obtain the balance equation

$$\frac{dr'}{dt} = \frac{M_B}{\rho_{SB} n_p} \frac{r_B V}{4\pi r'^2} \quad (33)$$

The number of particles is related to the initial mass and volume of B,

$$m_{0B} = n_p \frac{4}{3} \pi R^3 \rho_{SB} \quad (34)$$

The change of the radius becomes

$$\frac{dr'}{dt} = \left(\frac{R}{r'}\right) \frac{RM_B}{3m_{0B}} r_B V \quad (35)$$

When introduced by a dimensionless radius $y = r'/R$, eq 35 is described:

$$3y^2 \frac{dy}{dt} = \frac{M_B}{m_{0B}} r_B V \quad y = 1 \quad \text{at} \quad t = 0 \quad (36)$$

In an analogous manner it can be shown, that

$$2y \frac{dy}{dt} = \frac{M_B}{m_{0B}} r_B V \quad (37)$$

is valid for infinitely long cylinders and that

$$\frac{dy}{dt} = \frac{M_B}{m_{0B}} r_B V \quad (38)$$

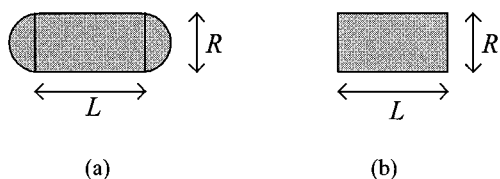
is valid for slabs. Furthermore, the equations can be generalized by introducing a form factor a :

$$\frac{a}{R} = \frac{A_{0p}}{V_{0p}} \quad (39)$$

where A_{0p} and V_{0p} denote the initial surface area and volume of the particle, respectively. The form factor is $a = 1$ for slabs and $a = 2$ for a long cylinder and $a = 3$ for spheres. Thus eqs 36, 37, and 38 can be compressed to

$$ay^{a-1} \frac{dy}{dt} = \frac{M_B}{m_{0B}} r_B V \quad (40)$$

Equation 40 can be used for arbitrary geometries provided, that the form factor can be estimated. The form factor is obtained from eq 39, provided that R , A_{0p} , and V_p can be evaluated from images of the particles. Two cases are considered: cylinders with half spherical ends and cut ends. The geometries are illustrated below.



By elementary geometric considerations it can be shown, that the form factors become

$$a = \frac{2(1 + 2R/L)}{1 + 4/3R/L} \quad \text{for (a)} \quad (41)$$

and

$$a = 2(1 + R/L) \quad \text{for (b)} \quad (42)$$

For computational purposes we introduce the substitution $z = y^a$, which gives $ay^{a-1} dy/dt = dz/dt$. Equation 40 is simplified to

$$\frac{dz}{dt} = \frac{M_B}{m_{0B}} r_B V \quad z = 1 \quad \text{at} \quad t = 0 \quad (43)$$

$$z \rightarrow 0 \quad \text{at} \quad t = \infty$$

De facto z is equal to the normalized mass of B: $z = m_B/m_{0B}$ that is, $z = (r'/R)^a$ and the radius r' at any moment of time is obtained from

$$r' = z^{1/a} R \quad (44)$$

The solid phase is described by eq 43 after which the radius is obtained from eq 44.

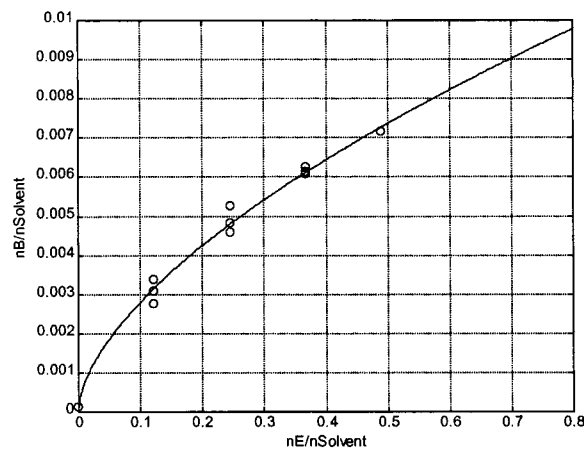


Figure 2. The relative solubility of methoxide (B) into chlorobenzene–methanol solution as a function of relative methanol concentration (E).

The SEM image (Figure 1) indicates that the particles might be well-represented as cylinders with half-spherical ends (case a, eq 41) and the ratio L/R being between 1 and 2. $L = 1$ gives $a = 2.57$ and $L = 2$ gives $a = 2.4$. Thus, the value of the form factor is not very sensitive for the L -to- R ratio. The average value $a = 2.5$ was chosen for calculations.

Summary of the Model Equations

The mathematical model for the system consists of the following equations:

$$1. \quad \frac{dn_A}{dt} = c_{0A} \dot{V} - rV \quad n_i = n_{0i} \quad \text{at} \quad t = 0$$

$$z = 1 \quad \text{at} \quad t = 0$$

$$2. \quad \frac{dn_C}{dt} = -rV$$

$$3. \quad \frac{dn_D}{dt} = +rV$$

$$4. \quad \frac{dn_E}{dt} = +2rV + \alpha r_{S2S3} V; \quad \alpha = (0, \dots, 1)$$

$$5. \quad \frac{dz}{dt} = -\frac{M_B}{m_{0B}} r_B V, \quad r' = z^{1/a} R, \quad z = \frac{m_B}{m_{0B}} = \frac{n_B}{n_{0B}}$$

The liquid-phase volume (V) is described with eqs 24a and 24b.

In case where the mass transfer of B is rapid and the film diffusion resistance is negligible, c_B^* can be directly replaced by c_B in the expression for r .

Experimental Procedures

Experimental Procedures for Solubility Measurements.

The measurements of sodium methoxide solubility in a mixture of chlorobenzene and methanol as solvents were carried out at 45–85 °C, and the methanol/chlorobenzene ratio was varied between 0 and 0.5. To the chlorobenzene–methanol solution in a flask (250 mL capacity) was quickly added solid sodium methoxide in an amount enough to keep the solid-phase always present. The flask was shaken

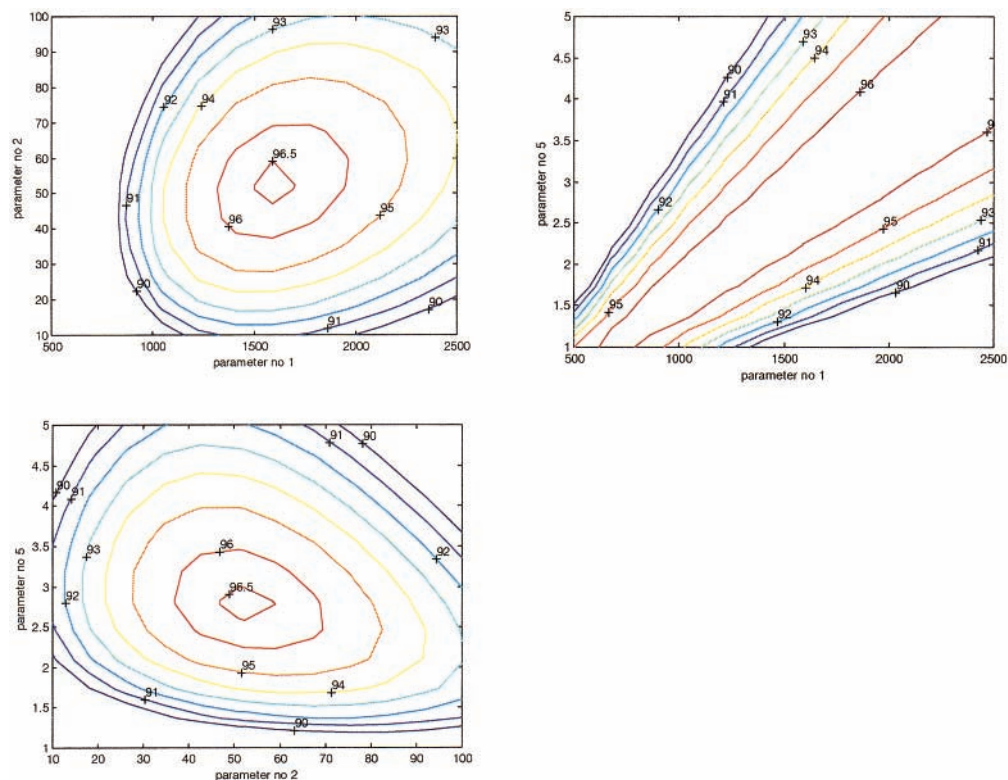


Figure 3. Maximum likelihood surface plots of parameters k_1 (parameter no. 1), k_{S2S3} (parameter no. 2), and lumped parameter K''' (parameter no. 5).

Table 1. Experimental variables

| | |
|-----------------|---|
| agitation speed | 300–450 rpm |
| temperature | 45–85 °C |
| A molar excess | 1.1–2.5 |
| B molar excess | 1.4 |
| A feeding time | 0.5–1 h |
| sampling | 0, 20, 40, 60, 90, 120, 180, 240, 300 min |

overnight in a thermostated water bath. The stirring was stopped, the solid phase was allowed to settle, and a sample was withdrawn from the solution through a filter using a preheated sampling device. The concentration of dissolved sodium methoxide was analyzed via a titrimetric method. The effect of the ketone on the solubility of sodium methoxide in chlorobenzene was not taken into account because of low concentration of the ketone in the system.

Experimental Procedure for Kinetic Measurements.

The kinetic experiments were carried out isothermally at atmospheric pressure in an automated reactor in a semibatch manner. The 2 dm³ jacketed glass reactor was equipped with a pitched blade turbine stirrer and a temperature probe. Temperatures were monitored and controlled by a personal computer (PC) equipped with data logging and control interfaces. The liquid reactant (A) was added using a peristaltic pump from a vessel on a balance, and the feed rate was monitored and controlled by the computer.

The reactor was purged with nitrogen prior to addition of the ester (C) dissolved in chlorobenzene. The agitation was started and solid sodium methoxide (B) was carefully charged into the reactor under nitrogen atmosphere to avoid contact with moist air. The kinetic experiments were carried

Table 2. Experimental conditions

| experiment no. | temperature °C | agitation speed (rpm) | A-feeding time (h) | A-excess | B-excess |
|----------------|----------------|-----------------------|--------------------|----------|----------|
| 1 | 85 | 450 | 1.0 | 1.1 | 1.4 |
| 2 | 85 | 300 | 1.0 | 1.1 | 1.4 |
| 3 | 55 | 300 | 1.0 | 1.1 | 1.4 |
| 4 | 45 | 300 | 1.0 | 1.1 | 1.4 |
| 5 | 45 | 300 | 0.5 | 1.1 | 1.4 |
| 6 | 45 | 300 | 1.0 | 1.1 | 1.4 |
| 7 | 45 | 300 | 1.0 | 1.4 | 1.4 |
| 8 | 45 | 300 | 1.0 | 1.1 | 1.4 |
| 9 | 75 | 300 | 1.0 | 1.1 | 1.4 |
| 10 | 65 | 300 | 1.0 | 1.1 | 1.4 |
| 11 | 75 | 300 | 1.0 | 1.8 | 1.4 |
| 12 | 75 | 300 | 1.0 | 2.5 | 1.4 |

Table 3. Estimated parameter values for the model system

| estimated parameter | parameter value | relative std error (%) |
|--|-----------------|------------------------|
| $k_1/(\text{dm}^3)^2 \text{ mol}^{-1} \text{ min}^{-1}$ | 1590 | 47.4 |
| $k_{S2S3}/(\text{dm}^3)^2 \text{ mol}^{-1} \text{ min}^{-1}$ | 52.1 | 4.7 |
| $E_1/\text{kJ mol}^{-1}$ | 56.4 | 2.9 |
| $E_{S2S3}/\text{kJ mol}^{-1}$ | 15.3 | 13.4 |
| $K'''/$ | 2.77 | 54.2 |

out isothermally at 45–85 °C. The ketone (A) was fed continuously at constant interval (0.5–1 h), and the reaction was continued for 5 h. Samples were withdrawn from the reaction mixture during the reaction and analyzed. No samples were taken from the gas phase. The effect of the agitation velocity on the mass transfer was investigated by

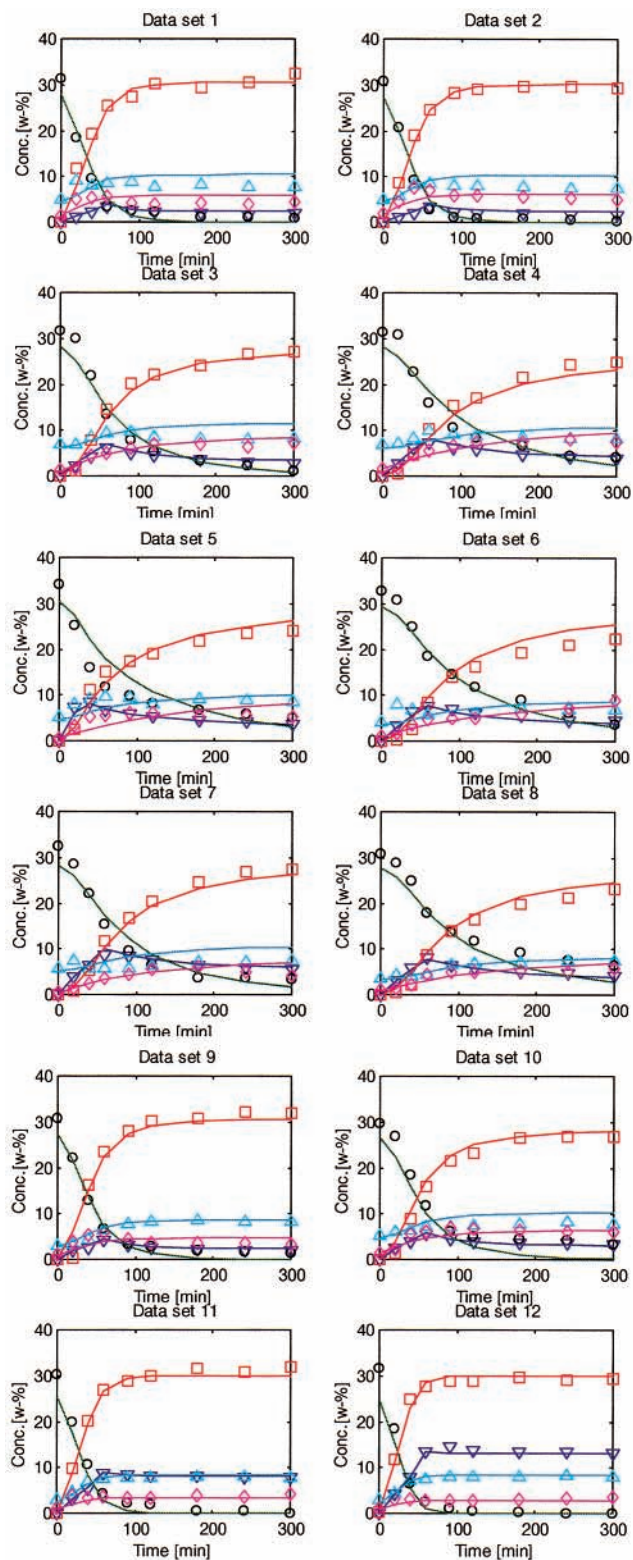


Figure 4. Comparison of experimental data and model simulation for data sets 1–12 (Table 2). Symbols: A (∇), C (\circ), D (\square), E (Δ), S21 (\diamond).

running the reaction at the stirring speed of 450 and 300 rpm. As it was found that reaction kinetics was not affected by stirring speed, all of the following experiments were conducted at the agitation speed of 300 rpm.

Chemicals. Commercial grade chemicals were used in the experiments. The key reactant carboxylic acid methylester

(C) was synthesized as a solution (1.39 mol/kg) with a small residual amount of dimethyl formamide and some methanol. The purities of sodium methoxide (B) and ketone (A) were 98.5 and 99.2%, respectively.

Analytical Methods. The compounds (C) and (D) liberated from the main reactions and the compounds S21, S41, and S42 from the side reactions were analyzed using high-pressure liquid chromatography (HPLC) and the compounds (A), (E), S51–S53 as well as the solvent concentration were determined with gas chromatography (GC).

Experimental Planning. See Tables 1 and 2.

Modelling Procedures and Results

Estimation Methods. The computations were performed using the MODEST software package (Haario, 1994). The MODEST (**MODEL ESTIMATION**) program package has been developed as an efficient tool to estimate parameters of mechanistic models as well as to design experiments and simulate and optimize model systems. The program code is written in Fortran 77.

The kinetic and reactor models were implemented in the subroutines of the program code. The mass balances, i.e., the ordinary differential equations (ODEs) were solved with the backward difference method for stiff (ODE) systems implemented in the LSODE software (Hindmarsh 1983). The weight fractions were calculated from the molar amounts and compared with the experimentally obtained weight fractions to find the optimal values of the kinetic parameters. The objective function was minimized with the hybrid simplex Marquardt–Levenberg method (Marquardt 1963). The objective function (Q) to be minimized was:

$$Q = \sum_t \sum_i (\hat{w}_{i,t} - w_{i,t})^2 \omega_i \quad (45)$$

where $\hat{w}_{i,t}$ denotes the weight fraction of a component (i) predicted by the model and $w_{i,t}$ is the experimental weight fraction at reaction time t . w_i is the weight factor of component (i). The weight factors, used to improve the identifiability of parameters in systems, which contain very different levels of measured concentrations, were set to 1 by default for all of the measurements in this case.

For the modelling purposes eq 14 was further simplified to improve the identifiability of the parameters in the estimation. By dividing the nominator and denominator in eq 18 with K' , we obtain after substitution

$$r = \frac{k_1 c_A c_B c_C}{c_C + K''' c_E} \quad (46)$$

The kinetic eq 46 was applied to the model for the main reaction scheme.

The lumped parameter K''' in eq 46 is given by

$$K''' = \frac{\left(\frac{1}{k_4 K_2 K_3} + \frac{1}{k_3 K_2} + k_2 \right) k_1}{K_1} \quad (47)$$

Solubility of Sodium Methoxide. The results of equilibrium solubility measurements of sodium methoxide (B)

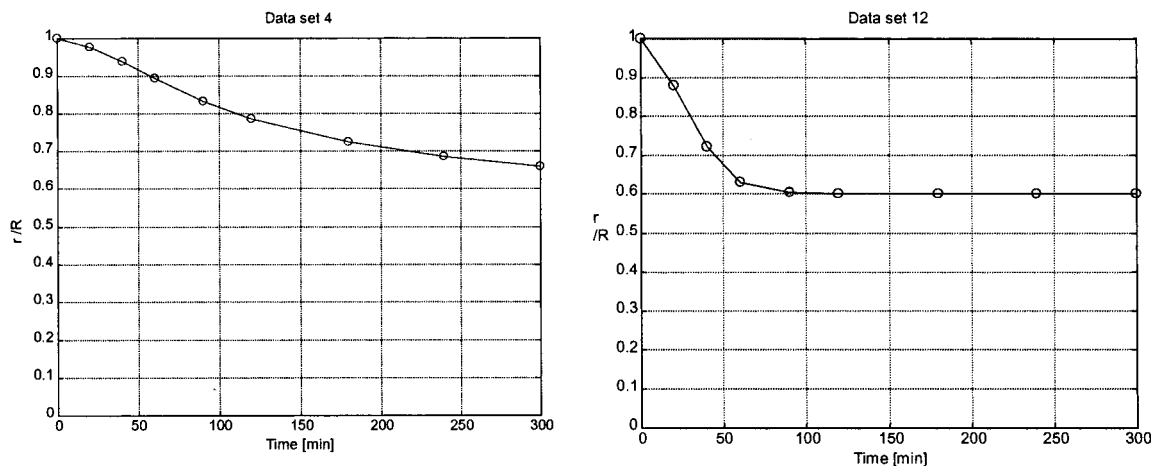


Figure 5. The dimensionless radius (r'/R) of the methoxide particles (form factor $a = 2.5$).

into chlorobenzene-methanol solution as a function of methanol (E) concentration in the solution are presented in Figure 2. The temperature had practically no effect to the solubility compared to the effect of methanol concentration at the temperature of 45–85 °C.

An empirical power-law function was introduced to describe the dependence of the methoxide solubility in chlorobenzene and methanol as a function of methanol concentration. Non-linear regression gave the following function, which was applied to kinetic data fitting to calculate an approximate non-mass transfer limited equilibrium solubility for methoxide (B)

$$n_B/n_{\text{Solvent}} = 0.949 \times 10^{-4} + 0.0111 \cdot (n_E/n_{\text{Solvent}})^{0.613} \quad (48)$$

Kinetic Modelling Results

All kinetic parameters and activation energies were fitted simultaneously. The proposed kinetic model for the semi-batch reaction system was able to predict the parameters reasonably well, the degree of explanation R^2 was about 97%. R^2 is defined as

$$R^2 = 1 - \frac{\sum_i (\hat{w}_i - w_i)^2}{\sum_i (w_i - \bar{w}_i)^2} \quad (49)$$

where \bar{w}_i is the average weight fraction of component (i).

The estimated parameter values and their relative standard errors (estimated standard error of the parameter divided by the estimated value of the parameter) are summarized in Table 3. The reference temperature for the rate constants (eq 19) was 45 °C. To keep the model as simple as possible K''' was taken independent of temperature.

A sensitivity analysis of model parameters as maximum likelihood surface contours (Green and Margerison, 1978) are presented in Figure 3. The mutual correlation between the parameters is low except between parameters k_1 and K''' . This is, however, explained by the structure of the model; since k_1 and K''' appear in the nominator and denominator, they have a compensating effect.

A summary of the fit of the model to individual experimental data sets is presented in Figure 4. A comparison between the data and the simulation shows no systematic deviations.

The dimensionless radius (r'/R) of the methoxide particles using a form factor of 2.5 for data sets 4 and 12 are presented as examples in Figure 5. The figures reveal that a considerable amount of unreacted methoxide remains in the system, which is in accordance with visual observations.

Conclusions

A kinetic model for an organic reaction system involving a sparingly soluble reactive solid phase was developed. Rate equations for consecutive linear reaction mechanisms using the pseudo-steady-state approximation for short-lived intermediates were applied on liquid–solid processes proceeding in an ideally mixed isothermal semibatch reactor. The reactions were considered as kinetically controlled reactions limited by the solubility equilibrium of the solid component. The dissolution rate of the reactive solid was regarded as non-mass transfer limited, i.e., so rapid that the solubility equilibrium always prevailed. No additional solid–liquid mass-transfer parameters were necessary in the solubility model. Different particle geometries of the solid were studied and a form factor concept was introduced in the kinetic modelling.

The model was applied to a Claisen condensation reaction as a case study, where the sparingly soluble reactive solid was sodium methoxide. The solubility equilibrium of methoxide into the reaction solvent was enhanced during the course of the reaction by methanol formed. The equilibrium solubility of methoxide was measured separately and a non-linear equilibrium solubility function approximated by experiments was applied to the model. The temperature effect on the solubility of methoxide, compared to the effect of the methanol concentration, was negligible in the experimental domain. The proposed model successfully described the experimental concentration data for the main components.

Acknowledgment

The authors are grateful to Dr. Elias Suokas for valuable discussions on the reaction mechanisms of this study.

Financial support from the Technology Development Centre (TEKES) is gratefully acknowledged.

Appendix: Notations in the Derivations of the Equations

$$a_1 = k_1 c_A c_B \quad (\text{A.1})$$

$$a_2 = k_2 c_C \quad (\text{A.2})$$

$$a_3 = k_3 \quad (\text{A.3})$$

$$a_4 = k_4 c_B \quad (\text{A.4a})$$

$$a_1 a_2 a_3 a_4 = k_1 k_2 k_3 k_4 c_A c_B c_C^2 \quad (\text{A.4b})$$

$$a_{-1} = k_1 \frac{c_E}{K_1} \quad (\text{A.5})$$

$$a_{-2} = \frac{k_2}{K_2} \quad (\text{A.6})$$

$$a_{-3} = k_3 \frac{c_B}{K_3} \quad (\text{A.7})$$

$$a_{-4} = k_4 \frac{c_D c_E}{K_4} \quad (\text{A.8})$$

$$a_{-1} a_{-2} a_{-3} a_{-4} = \frac{k_1 k_2 k_3 k_4}{K_1 K_2 K_3 K_4} c_E^2 c_B c_C \quad (\text{A.9})$$

NOTATION

| | |
|----------------------|--|
| A | mass transfer area |
| a | form factor |
| a_{-1}, \dots, a_4 | auxiliary variable (eqs 6–9), the Appendix |
| c | concentration |
| E | activation energy |
| K | equilibrium constant |
| K', K'', K''' | lumped parameters |
| k | rate constant |
| k_L | liquid-phase mass transfer coefficient |
| L | length of particle |
| M | molar mass |
| m | mass |
| N | flux |
| n | molar amount of substance |
| n_p | number of particles |
| \dot{n} | molar flow |

| | |
|---|---|
| Q | objective function |
| R | initial radius of particle |
| R_g | gas constant |
| r | reaction rate |
| r' | particle radius |
| $r_A, r_B, r_C,$ $r_D, r_E,$ | generation/consumption rate of compound |
| T | temperature |
| T_0 | reference temperature |
| t | time |
| V | volume |
| \dot{V} | volumetric flow rate |
| w | weight fraction |
| y | dimensionless particle radius |
| z | transformed variable ($z = y^d$) |

Greek letters

| | |
|----------|----------------------------|
| ν | stoichiometric coefficient |
| ρ | density |
| ω | weight factor |

Subscripts and Superscripts

| | |
|-----|----------------------------|
| i | component index |
| j | reaction index |
| L | liquid phase |
| p | particle |
| S | solid phase |
| 0 | inlet or initial condition |
| * | saturated state |

Abbreviations

| | |
|---------|--|
| Ar- | aromatic ring |
| A–E | reaction components |
| A1–A4 | reaction components (intermediates in the reactions) |
| B | solid compound |
| R- | aliphatic |
| S11–S53 | reaction components and intermediates (side reactions) |

Received for review February 17, 2000.

OP0000172